Lattice Dynamics of Zn-Cd Chalcogenides—A Critical-Point Analysis

D. N. Talwar and Bal K. Agrawal
Department of Physics, University of Allahabad, Allahabad-211002, India
(Received 19 October 1972)

The frequency–wave-vector dispersion relations for the normal modes of vibrations for zinc and cadmium tellurides, crystallizing in the zinc-blende crystal structure, have been calculated in the framework of the second-neighbor-ionic model. The frequencies of four critical-point phonons [LO(Γ), TO(Γ), LO(X), and TA(X)] obtained by infrared- and Raman-scattering measurements and the three elastic constants c_{11}, c_{12}, and c_{44} have been employed as input data so as to calculate the involved seven lattice-dynamical model parameters. Absorption maxima in the infrared and/or second-order Raman-scattering experiments have been tentatively assigned by an extensive use of the lattice-dynamical-calculated critical phonons. The calculated phonon frequencies show a reasonably satisfactory agreement with the available optical data.

I. INTRODUCTION

Similar to III-V compounds most of the II-VI-group semiconductors also crystallize in the zinc-blende crystal structure and have aroused a good deal of interest over the past few years. The interest in both theoretical and experimental studies of these compounds has been renewed because of their relatively simple crystal structure. One may interpret easily the experimental measurements with the aid of available oversimplified theoretical models. Just after the advent of coherent-inelastic neutron scattering experiments, extensive data of phonon spectrum in the various zinc-blende crystals[1–7] have been accumulated in recent years. Except for ZnSe[4] the neutron scattering data for the phonon spectrum in many of the II-VI-group semiconductors are still unavailable. However, a lot of the information regarding the phonon spectrum for the II-VI compounds, such as zinc and cadmium tellurides, can be gathered with the aid of the physically significant theoretical models.

The theory of lattice dynamics for the compounds having zinc-blende crystal structure has been discussed with the phenomenological shell and rigid-ion models. In shell-model[8] calculations, the polarizability of the ions is accounted for by considering both core and shell interaction between the respective ions. Also, one utilizes the fact that the short-range overlap force between ions depends on their state of polarization, and conversely. The model has been utilized by various authors to calculate the phonon dispersion curves in GaAs, [1] GaP, [2] and InSb. [5] The shell model, although it gives a reasonable agreement with the neutron work, requires a heavy computation and an interpolation of a rather large number of fitting constants, and is meaningful only when detailed inelastic neutron scattering data are available. It is certain from the evidence available for the hybrid nature of the bond in zinc-blende crystals[9] that an appreciable contribution to the bond is ionic in character. The rigid-ion model (RIM) and its various ramifications have a general applicability to the system of solids, and they also have many computational advantages over that of the shell model. Also, it produces qualitatively good results. A RIM, in general, incorporates the short-range-force model of Smith[10] for a diamond structure, and the long-range-Coulomb-force model introduced by Kellerman[11] for an ionic crystal having the rocksalt structure.

Rajagopal and Srinivasan[12] introduced a four-parameter RIM to study the dispersion relations, the frequency-distribution function, and the specific heat of zinc sulphide. The model has been abundantly used by Vetelino and Mitra[13] and by Vetelino *et al.* [14,15] for studying the lattice dynamics and the thermodynamical properties of SiC, ZnS, and ZnTe. However, marked discrepancies have been observed in their results, particularly for zone-boundary phonons. [15] In an effort to improve the results of the four-parameter RIM, Banerjee and Varshni[16] have presented a physically meaningful and most economical (as regards the number of parameters) seven-parameter second-neighbor-ionic (SNI) model. They successfully used the model to match the observed neutron data in GaAs, [16] ZnS, and GaP, [17] and also discussed the thermodynamical properties of various III-V and II-VI compounds. Earlier we employed their SNI model to calculate the phonon dispersion curves for ZnSe, InSb, [18] and CuI, [19] and have obtained a reasonable agreement with the recently available neutron scattering results. [4,5,7]

This paper is devoted to applying the SNI lattice-dynamical model to calculate the phonon dispersion curves along the high-symmetry [(ξ, 00), (0, ξ, ξ), and (ξ, ξ, ξ)] directions in zinc and cadmium tellu-

rides. The reliability of the calculated phonons has been tested by comparing the obtained values for the critical-point-phonon frequencies with the neutron scattering data for various compounds having ZnS structure, and also by examining the applicability of the available Brout sum rule.[20] An extensive use of the calculated critical-point phonons is then made successfully to assign the absorption peaks observed in infrared and/or second-order Raman spectrum.

II. LATTICE DYNAMICS

In the lattice dynamical SNI model, we consider the short-range-force model up to and including second neighbors along with the long-range Coulomb forces. The equations of motion in the harmonic approximation in matrix form for an ionic crystal can be written

$$\omega^2 \overleftrightarrow{m}\,\vec{u} = \overleftrightarrow{D}^{sC}\vec{u}\ , \tag{1}$$

where $\overleftrightarrow{m}$ is the diagonal matrix formed by m_κ, the masses of the two atoms in the unit cell; $\vec{u}$ is the eigenvector column matrix, and $\overleftrightarrow{D}^{sC}$ is the dynamical matrix containing the short-range (non-Coulomb) part D^s and the Coulomb part D^C. The secular equation determining the angular frequencies ω of the normal modes of vibration is

$$\left|\omega^2 \overleftrightarrow{m}\ \overleftrightarrow{1} - \overleftrightarrow{D}^{sC}\right| = 0. \tag{2}$$

In order to solve these equations, one must construct $D^{sC}_{xy}(\vec{q};\ \kappa,\ \kappa')$, the elements of the dynamical matrix in the reciprocal space ($\vec{q}$ is the wave vector).

Applying the symmetry properties of the zinc-blende crystal lattice,[21] the dynamical matrix elements for the short-range interactions are described by the first-neighbor (α, β) and second-neighbor (μ_κ, ν_κ, λ_κ, and δ_κ) force constants. The number of parameters can be reduced by taking μ equal to ν in concurrence with the central-force model of Smith.[10] In the SNI model[16] the diagonal and nondiagonal elements of $D^s(\vec{q};\ \kappa,\ \kappa')$ are

$$D^s_{xx}(\vec{q};\ \kappa,\ \kappa) = 4[\alpha + \lambda_\kappa(1 - \cos\pi q_y \cos\pi q_z) + \mu_\kappa(2 - \cos\pi q_x\cos\pi q_y - \cos\pi q_z\cos\pi q_x)], \tag{3}$$

$$D^s_{xy}(\vec{q};\ \kappa,\ \kappa) = 4(\mu_\kappa \sin\pi q_x \sin\ q_y) = D^s_{yx}(\vec{q};\ \kappa,\ \kappa)\ , \tag{4}$$

$$D^s_{xx}(\vec{q};\ \kappa,\ \kappa') = -\alpha(e^{i\pi(a_x+a_y+a_z)/2} + e^{i\pi(a_z-a_x-a_y)/2} + e^{i\pi(a_y-a_x-a_z)/2} + e^{i\pi(a_x-a_y-a_z)/2}), \tag{5}$$

$$D^s_{xy}(\vec{q};\ \kappa,\ \kappa') = -\beta(e^{i\pi(a_x+a_y+a_z)/2} + e^{i\pi(a_z-a_x-a_y)/2} - e^{i\pi(a_y-a_x-a_z)/2} - e^{i\pi(a_x-a_y-a_z)/2}) = D^s_{yx}(\vec{q};\ \kappa,\ \kappa')\ . \tag{6}$$

The other elements can be obtained by a cyclic permutation of the indices and by using the fact that

$$D^s_{xy}(\vec{q};\ \kappa,\ \kappa') = D^{s*}_{xy}(\vec{q};\ \kappa',\ \kappa)\ ,$$

where $D^{s*}_{xy}(\vec{q};\ \kappa,\ \kappa')$ is the complex conjugate of $D^s_{xy}(\vec{q};\ \kappa,\ \kappa')$.

The expressions for the long-range or the Coulomb coefficients $D^C(\vec{q};\ \kappa,\ \kappa')$ originally given by Kellerman[11] for rocksalt structure have been modified by Cochran[8] for the diamond structure, and by Merten[21] for the zinc-blende lattice. The diagonal and nondiagonal elements of the Coulomb coefficients $D^C(\vec{q};\ \kappa,\ \kappa')$ for the zinc-blende crystal structure are as follows[12,16]: for $\vec{q} = 0$,

$$D^C_{xy}(\vec{q};\ \kappa,\ \kappa') = \tfrac{2}{3}\pi\chi\delta_{xy}\ ; \tag{7}$$

for $\vec{q} \neq 0$,

$$D^C_{xy}(\vec{q};\ \kappa,\ \kappa) = \tfrac{1}{2}\chi[-G_{xy}(\kappa,\ \kappa) + H^{\vec{l}}_{xy} + (8/3\sqrt{\pi})\,\epsilon^3\delta_{xy}], \tag{8}$$

$$D^C_{xy}(\vec{q};\ \kappa,\ \kappa') = \tfrac{1}{2}\chi[G_{xy}(\kappa,\ \kappa') - H^{\vec{m}}_{xy}], \tag{9}$$

with $\chi = Z^2e^2/a^3$ and

$$G_{xy}(\kappa,\ \kappa) = 4\pi \sum_{\vec{h}} \frac{(h_x+q_x)(h_y+q_y)}{(\vec{h}+\vec{q})^2} \times \exp\left(-\frac{\pi^2}{4\epsilon^2}(\vec{h}+\vec{q})^2\right),$$

$$G_{xy}(\kappa,\ \kappa') = 4\pi \sum_{\vec{h}} \frac{(h_x+q_x)(h_y+q_y)}{(\vec{h}+\vec{q})^2} \times \exp\left(-\frac{\pi^2}{4\epsilon^2}(\vec{h}+\vec{q})^2\right) \times \exp\left(-\frac{i\pi}{2}(h_x+h_y+h_z)\right),$$

$$H^{\vec{l}}_{xy} = 2\sum_{\vec{l}}[-f(\vec{l})\,\delta_{xy} + g(\vec{l})\,l_x l_y/\vec{l}^{\,2}]\cos\pi\vec{q}\cdot\vec{l}\ ,$$

$$H^{\vec{m}}_{xy} = 2\sum_{\vec{m}}[-f(\vec{m})\,\delta_{xy} + g(\vec{m})\,m_x m_y/\vec{m}^2]\,e^{i\pi\vec{q}\cdot\vec{m}}\ ,$$

$$f(\vec{l}) = \frac{2\epsilon}{\sqrt{\pi}}\,\frac{e^{-\epsilon^2\vec{l}^2}}{\vec{l}^2} + \frac{\psi(\epsilon\vec{l})}{\vec{l}^3}\ ,$$

$$g(\vec{l}) = 3f(\vec{l}) + (4\epsilon^2/\sqrt{\pi})\,e^{-\epsilon^2\vec{l}^2}\ ,$$

and

$$\psi(\epsilon\vec{l}) = 1 - (2/\sqrt{\pi})\int_0^{\epsilon\vec{l}} e^{-t^2}dt\ .$$

Here ϵ is an arbitrary parameter generally taken to be unity; $\vec{l} \equiv (l_x,\ l_y,\ l_z)$ and $\vec{m} \equiv (m_x,\ m_y,\ m_z)$ are the lattice vectors, and $\vec{h} \equiv (h_x,\ h_y,\ h_z)$ is the reciprocal-lattice vector. For details, we refer to the Ref. 16.

III. CALCULATION OF THE PARAMETERS

In order to calculate the phonon dispersion curves along the symmetry directions, Rajagopal and Srinivasan[12] have evaluated the four unknown parameters α, β, μ, and Z by employing the three

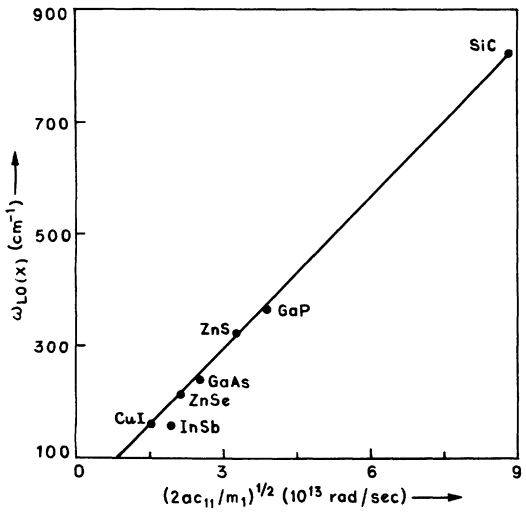

FIG. 1. A plot for the longitudinal-optical-phonon frequency [LO(x)] at the zone-boundary in units of cm^{-1} versus $(2ac_{11}/m_1)^{1/2}$ for various compounds having zinc-blende crystal structure. Solid dots (●) are the experimental points due to the measurements of Hennion *et al.* for CuI and ZnSe (Refs. 7 and 4); of Price *et al.* for InSb (Ref. 5); of Waugh and Dolling for GaAs (Ref. 1); of Yarnell *et al.* for GaP (Ref. 2); of Feldkamp *et al.* for ZnS (Ref. 3); and of Feldman *et al.* for SiC [D. W. Feldman, J. H. Parker, Jr., W. J. Choyke, and L. Patrick, Phys. Rev. 173, 787 (1968)].

expressions for the elastic constants and an expression obtained after taking an average of the two long-wavelength [LO(Γ) and TO(Γ)] phonons. This procedure, in fact, does not produce a proper splitting of phonon frequencies neither at the zone center nor at the zone boundary, and it also produces an unrealistic value for the effective charge. Vetelino *et al.* [13–15] took an alternative step and determined the four parameters by relating them to the elastic constants and the zone-center-phonon [LO(Γ) and TO(Γ)] frequencies. They then solved, in the least-squared sense, the obtained five equations involving four unknowns. They were able to exactly reproduce the zone-center phonons, but marked discrepancies were seen to exist especially for the zone-boundary-phonon frequencies.

In their seven-parameter lattice-dynamical model, Banerjee and Varshni[16] have deviated from the usual procedure of calculating the unknown parameters. They employed critical-point phonons (determined by optical measurements) as input data, and employed the three experimentally determined elastic constants as constraint on the calculated values of the parameters. These authors have successfully explained the dispersion relations for various III-V and II-VI semiconductors compounds. As mentioned earlier, as no detailed neutron scattering data are available for these crystals at this time, we therefore do not possess the exact critical-phonon frequencies for the evaluation of the seven parameters in this model. We have, thus, adopted an alternative approach to seek a guideline for the critical-point-phonon frequencies.

The principal information regarding the transverse-optical TO(Γ) and the longitudinal-optical LO(Γ) modes for the long-wavelength vibrations can be had from the study of infrared reflection or absorption spectrum, [22–41] first- or second-order Raman scattering on bulk samples[42–46] or from the analysis of the band-edge emission spectrum. [47] Quite recently Beserman and Balkanski[22] have observed the zone-center-phonon frequencies in the infrared reflection spectrum for ZnTe and CdTe crystals. These frequencies were in close agreement with those measured by first-order Raman scattering and from the analysis of the band-edge emission spectrum.

A correct analysis to get critical-point phonons at the zone boundaries of the Brillouin zone from the optical measurements (infrared or Raman spectrum) can be performed either by suitably interpreting the absorption peaks in terms of the combination of two, three, or more characteristic LO, LA, TO, and TA phonons, or more directly by a comparison with the neutron scattering results. In the absence of the neutron data, however, approximate values of the longitudinal-optical-[LO(X)] or longitudinal-acoustic- [LA(X)] phonon frequencies at the zone boundary can be determined by plotting values of these phonons obtained by the neutron or Raman-scattering measurements as a function of $(2ac_{11}/m_1)^{1/2}$ or $(2ac_{11}/m_2)^{1/2}$ for various compounds having zinc-blende crystal structure (see Figs. 1 and 2). Here $2a$ is the lattice constant, c_{11} is one of the experimentally determined elastic constants, and m_1 is the mass of the lighter atom ($m_1 < m_2$). Both of these curves are found to be approximately linear. For ZnTe and CdTe, the calculated values of $(2ac_{11}/m_1)^{1/2}$ are 1.99 and 1.38×10^{13} rad/sec, while those of $(2ac_{11}/m_2)^{1/2}$ are 1.47 and 1.25×10^{13} rad/sec, respectively. These values in turn, give LO(X) = 185 cm^{-1}, LA(X) = 140 cm^{-1} for ZnTe and LO(X) = 153 cm^{-1}, LA(X) = 102 cm^{-1} for CdTe. Furthermore, the measurements of the second-order Raman spectrum using a laser source of excitation, promises to give quite accurate and complementary information to that of the infrared reflectivity or absorption measurements in many cases. Recently, Irwin and LaCombe[44] have observed a peak at 364 cm^{-1} by second-order Raman scattering for ZnTe while the same was missing in the infrared spectrum measured earlier by Narita *et al.* [25] Their assignment for that peak [2LO(X)] again seems to be worthwhile, as this type of combination (according to Birman's selection rules[48]) is

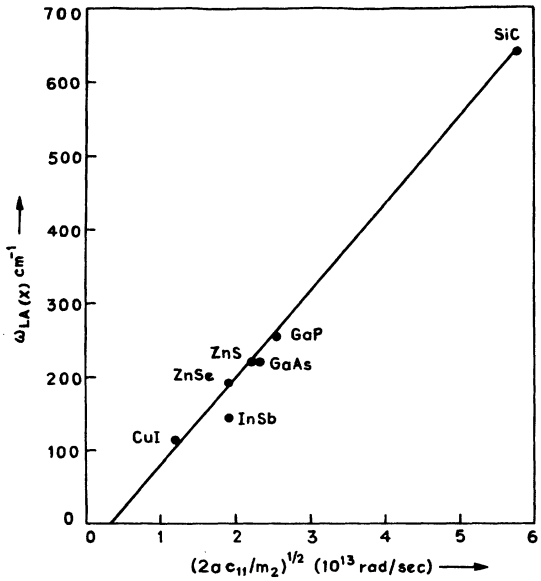

FIG. 2. A plot for the longitudinal-acoustic-phonon frequency [LA(x)] at the zone boundary in the units of cm^{-1} versus $(2ac_{11}/m_2)^{1/2}$ for various zinc-blende compounds. Solid dots (●) are the experimental points.

forbidden in infrared absorption, but is allowed in Raman scattering. Our theoretically calculated value for the LO(X) (= 185 cm^{-1}) phonon also lends support to their assignment. Quite recently, Slack and Roberts[49] have given a reasonably reliable assignments for acoustic phonons from the far-infrared absorption measurements for the various admantine crystals. They have compared their results as a check with those of the neutron data where available, and have found a good agreement.

In the calculation of the involved parameters for ZnTe and CdTe, we have deviated a bit from the procedure of Banerjee and Varshni. As an input data we employ the frequencies of four phonons LO(Γ), TO(Γ), LO(X), and TA(X) (available from the optical measurements) and the three elastic constants c_{11}, c_{12}, and c_{44}. The approximate values of the frequencies of TO(X) and LA(X) phonons were calculated from the Brout sum rule[20] using the known values of the phonon frequencies at the center and at the boundary of the Brillouin zone. These values are used as a check on the calculated parameters. As usual, two of the parameters α and χ are calculated using the LO(Γ)- and TO(Γ)-phonon frequencies. The parameter μ_1 is calculated using LO(X) phonon frequency, while μ_2 is calculated with the aid of the elastic constant c_{11} in such a way that it should reproduce a reasonable value of LA(X). Approximate values of β and $(\lambda_1+\lambda_2)$ are then calculated from the remaining two elastic constants c_{12} and c_{44}. Values of β, λ_1, λ_2, and TO(X) are then varied slightly to get the observed value of TA(X). During this fitting procedure, due attention has been paid to keep the differences between the observed and the calculated elastic constants within the limit of experimental error.

The macroscopic data used in the calculations of the unknown parameters along with the calculated parameters for ZnTe and CdTe are presented in Table I. The calculated phonon dispersion curves along high symmetry [$(\xi, 0, 0)$, $(0, \xi, \xi)$, and (ξ, ξ, ξ)] directions are displayed in Figs. 3 and 4, respectively.

IV. CRITICAL-POINT ANALYSIS OF THE INFRARED AND/OR RAMAN-SCATTERING PHONON BANDS

The experimental results from the observed infrared and/or second-order Raman bands bear insufficient knowledge to decide which possible combinations of the critical-point phonons give rise to a particular peak in the observed spectrum. An exact interpretation of the observed spectrum in terms of the critical phonons is quite straightforward if the phonon frequencies at critical points in the Brillouin zone are available by neutron scattering experiments.[50] In the absence of neutron data, however, some plausible assignments as to the shape and the approximate positions of the

TABLE I. Experimental and theoretical values of macroscopic quantities: Phonon frequencies are in units of cm^{-1}. Elastic constants are in units of 10^{11} dyn/cm^2. All the lattice-dynamical-model parameters α, β, μ_1, μ_2, λ_1, λ_2, and χ are in units of 10^3 dyn/cm.

	ZnTe		CdTe	
Quantity	Expt.	Theor.	Expt.	Theor.
LO(Γ)	208.5[a]		167[a]	
TO(Γ)	177[a]		139[a]	
LO(X)	182[b]		152[c]	
TA(X)	55[d]		35[d]	
c_{11}	7.13[e]		5.351[f]	
c_{12}	4.07[e]		3.681[f]	
c_{44}	3.12[e]		1.994[f]	
α		22.6307		19.553
β		22.4		20.5
μ_1		1.6848		4.1676
μ_2		3.3723		−0.5475
λ_1		−6.23		0.12217
λ_2		3.9		−3.2859
χ		4.825		4.8072

[a]Reference 22.
[b]Reference 44.
[c]Reference 45.
[d]Reference 49.
[e]D. Berlincourt, H. Jaffe, and L. R. Shiozawa, Phys. Rev. 129, 1009 (1963).
[f]H. J. McSkimm and D. G. Thomas, J. Appl. Phys. 33, 56 (1962).

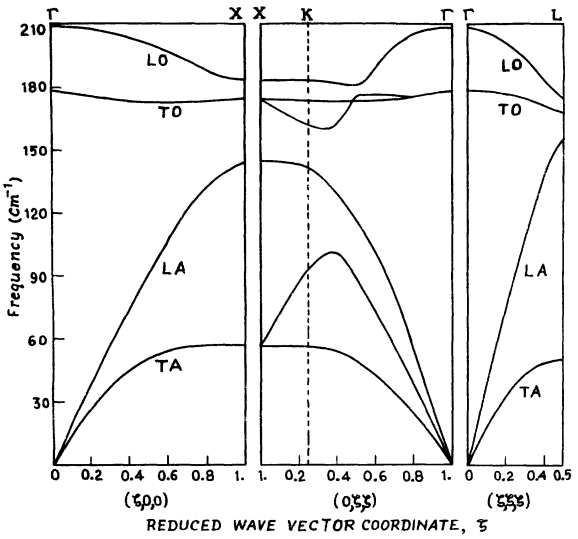

FIG. 3. Calculated phonon dispersion curves for ZnTe in the $(\xi, 0, 0)$, $(0, \xi, \xi)$, and (ξ, ξ, ξ) directions. The phonon frequencies are in units of cm^{-1}. The letters Γ, X, K, and L refer to the symmetry points in the Brillouin zone, and $\xi (= \tilde{q}/\tilde{q}_{max})$ is the reduced wave-vector coordinate.

bands observed in infrared or Raman spectrum due to critical-point phonons have been wrongly made by some authors for ZnTe,[25,26] CdTe,[32,45] and ZnSe.[51]

From a space-group analysis, Birman[48] has worked out the selection rules for the allowed two- and three-phonon absorption bands for the diamond and zinc-blende crystal structures at the critical points. We made an extensive use of the approximate results of the lattice-dynamical model and the observed acoustic phonons by far-infrared measurements as a guide so as to make tentative assignments (Tables II and III) for the multiphonon peaks of the optical spectra in terms of the characteristic phonons. In the assignments, we have kept in mind the selection rules for the transitions and also the intensity of the observed absorption peaks. The phonon peaks with a relatively higher intensity are considered to be constructed by two-phonon processes, whereas the lower intensity peaks arise because of the three-phonon processes.[52]

The selected critical-point phonons that reproduce the observed peaks of the infrared and/or Raman spectrum to an accuracy of four wave numbers agree reasonably well with the results of our lattice-dynamical calculations. The only discrepancy observed in the present case, particularly for the TA(L) phonon for ZnTe, is similar to that obtained earlier in GaAs,[16] ZnS-GaP,[17] InSb-ZnSe,[18] and CuI[19] while comparing the theoretical results with the neutron data. In order to have a futher support for the calculated lattice-dynamical results, we have collected data for the various optical measurements from the literature and have reproduced it for ZnTe, CdTe, and InSb in Table

TABLE II. Assignment of the absorption peaks observed by infrared and second-order Raman scattering for ZnTe in terms of two- and three-phonon processes. Selected critical-point-phonon frequencies (cm^{-1}) for the edges of the zone that reproduce the observed spectra are compared with the lattice-dynamical calculations.

	Γ		X		L	
Phonon branch	Selected	Calc.	Selected	Calc.	Selected	Calc.
LO	208	208.5	182	183	175	174
TO	178	178	175	174	172	170
LA			142	144	156	152
TA			55	55	39	47

Infrared peak positions (cm^{-1}) Ref. 25	Assignments	Second-order Raman peak positions (cm^{-1}) Ref. 44	Calc. (cm^{-1})
···	TA(X) + LO(X)	240	237
253	2TA(L) + TO(X); or 2TA(X) + LA(X)	···	253
282	2LA(X)	282	284
289	2TA(X) + TO(Γ)	290	288
302	···	300	···
313	2LA(L)	310	312
332	LO(L) + LA(L)	329	331
337	2LA(X) + TA(X); or 2TO(L)	340	339
351	2TO(X) or 2LO(L)	349	350
359	TO(Γ) + LO(X)	358	360
···	2LO(X)	364	364
374	TA(X) + TO(Γ) + LA(X)	···	374
380	TA(X) + LA(X) + LO(X)	···	379
387	LO(L) + LA(L) + TA(X)	···	386
403	TA(L) + LA(L) + LO(Γ)	···	403
410	TO(X) + TA(X) + TO(Γ)	···	408
414	2LO(Γ)	412	416
423	TA(L) + LO(L) + LO(Γ)	···	423
435	TO(X) + TA(X) + LO(Γ)	···	438
444	TA(X) + LO(Γ) + LO(X)	···	445
458	2LA(X) + TO(X)	···	459
465	2LA(X) + LO(X)	···	466
476	LO(L) + LA(L) + LA(X)	···	473

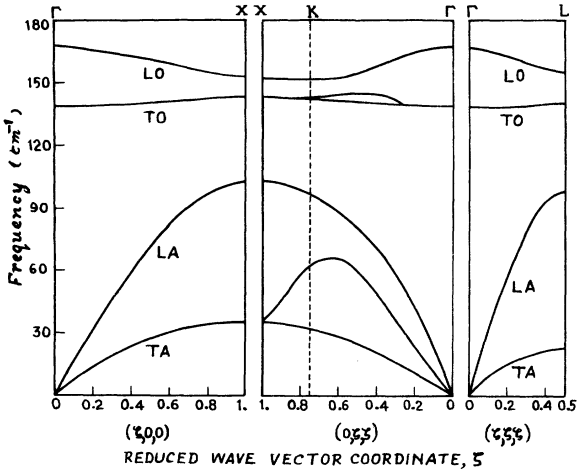

FIG. 4. Calculated phonon dispersion curves for CdTe in the $(\xi, 0, 0)$, $(0, \xi, \xi)$, and (ξ, ξ, ξ) directions. The phonon frequencies are in the units of cm^{-1}. The letters Γ, X, K, and L refer to the symmetry points in the Brillouin zone.

TABLE III. Assignment of the absorption peaks observed by infrared and Raman scattering for pure CdTe in terms of two-phonon processes. Selected critical-point phonons (cm^{-1}) for the edges of the zone that reproduce the observed spectra are compared with the lattice-dynamical calculations.

	Γ		X		L	
Phonon branch	Selected	Calc.	Selected	Calc.	Selected	Calc.
LO	167	167	153	153	152	156
TO	139	139	143	143	140	140
LA			101	103	104	100
TA			36	35	25	24

Infrared peak positions (cm^{-1})				Raman peak positions (cm^{-1})	
Ref. 36	Ref. 35	Ref. 45	Assignments	Ref. 45	Calc. (cm^{-1})
...	...	...	$LA(X) - LA(X)$	61	65
71	74	74	$2TA(X)$	72	72
...	...	...	$TO(X) - TA(X)$	105	107
114	115	115	$TO(L) - TA(L)$	114	115
...	...	...	$TO(\Gamma)$	140	139
...	...	...	$LO(\Gamma)$	171	167
...	...	...	$LO(X) + TA(X)$	186	189
...	...	...	$2LA(X)$	203	202
208	...	...	$2LA(L)$	...	208
247	...	...	$TO(X) + LA(X)$; or $TO(L) + LA(L)$	...	244
253	250	250	$LO(X) + LA(X)$	...	254
293	290	290	$LO(L) + TO(L)$	...	292
304	302	300	$2LO(L)$	...	304

TABLE IV. Infrared absorption data for acoustic and optical phonons in pure ZnTe, CdTe, and InSb. The corresponding Raman- and neutron scattering data, if available, have been presented and the lattice-dynamical calculated phonons are given. All the phonons frequencies are in cm^{-1}.

	Infrared absorption and other optical data	Raman-scattering data	Neutron scattering data	Lattice-dynamical calculations		
System				SNI model calculation	Ref. 15	Lattice mode assignments
ZnTe	206–208.5[a]	203–208.3[b]		208.5	206	$LO(\Gamma)$
	177–179[a]	177[b]		178	179	$TO(\Gamma)$
	180[a]	182[b]		183	190	$LO(X)$
	110[a]	107[b]		110	168	$2TA(X)$
	84[a]	...		94	116	$2TA(L)$
	156[a]	...		157	138	$LA(L)$
CdTe	167–178[c]	171[d]		167		$LO(\Gamma)$
	139–145[c]	140[d]		139		$TO(\Gamma)$
	150–153[c]	150[d]		153		$LO(X)$
	71–72[c]	72[d]		70		$2TA(X)$
	50[c]	71[d]		48		$2TA(L)$
	104–104.3[c]	...		100		$LA(L)$
InSb	197[e]	191[f]	197[g]	197		$LO(\Gamma)$
	184.7–187[e]	180[f]	185[g]	185		$TO(\Gamma)$
	159.6[e]	...	158.5[g]	158.5		$LO(X)$
	84[e]	...	75[g]	73		$2TA(X)$
	68[e]	...	66[g]	56		$2TA(L)$
	136[e]	...	127[g]	125		$LA(L)$

[a]References 22–29. [b]References 42–44. [c]References 22, 30–39. [d]Reference 45. [e]References 40 and 41. [f]References 42 and 46. [g]Reference 6.

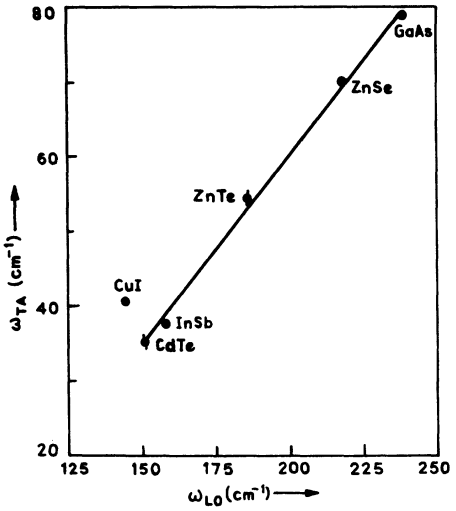

FIG. 5. Values of the longitudinal-optical frequency versus transverse-acoustic frequency at the zone boundary for various zinc-blende compounds. Solid dots (●) refer to the experimental points, whereas the points (ϕ)for ZnTe and CdTe are the lattice-dynamically calculated values.

IV. For comparison, the lattice-dynamical results for ZnTe obtained by Vetelino *et al.*,[15] are also reproduced in Table IV. Their results, particularly for the zone-boundary phonons are found to be much different from our results and the optical data. Again, since InSb has a zinc-blende structure and the masses of its atoms are very

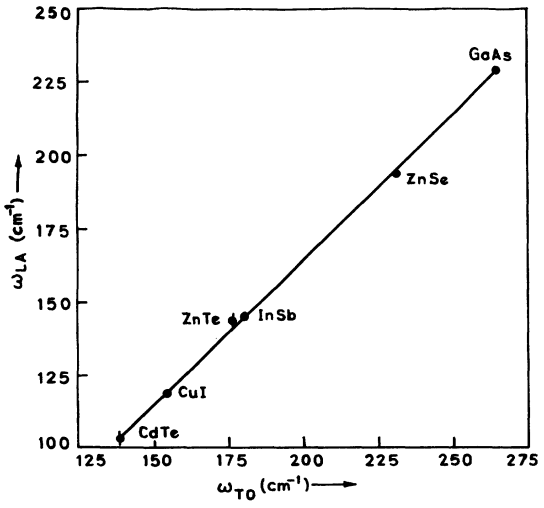

FIG. 6. Values of the longitudinal-acoustic frequency versus transverse-optical frequency at the zone boundary for various zinc-blende compounds. Solid dots (●) refer to the experimental points, whereas the points (ϕ) for ZnTe and CdTe are the lattice-dynamically calculated values.

much similar to that of CdTe, it is therefore worthwhile to compare the critical-point phonons for InSb recently observed in the neutron scattering measurements by Price *et al.*[5] with those calculated for CdTe. From Table IV it is evident that the LO(X), TA(L), and TA(X) phonons for CdTe calculated by SNI model are in reasonable agreement with that of the neutron data for InSb, thus lending support to the employed lattice-dynamical model.

In order to have a further check of the reliability of the analyzed frequencies, we follow the procedure of Mitra and Marshall[53] in plotting the interrelations (Figs. 5 and 6) between the optical and acoustical phonon frequencies at the zone boundaries in various zinc-blende-type compounds. In these plots, we have also quoted the neutron data available for most of the systems. The regularity of the curves for ZnTe and CdTe with neutron results support, once again, the calculated zone-boundary optical- and acoustical-phonon frequencies .

The calculated LO and TO zone-boundary-phonon frequencies for ZnTe and CdTe suggest that the two branches do not cross at the zone boundaries. It can be checked with the aid of Szigetti's[54] semiempirical relation for the degree of ionicity. Keyes[55] has investigated that if the two highest characteristic phonon frequencies were labeled ω_{LO} and ω_{TO} in a proper order for various zinc-blende-type compounds, then $(\omega_{LO}/\omega_{TO})^2$ would be a linear function of $(q_{eff}/e)^2$. The Szigetti effective charge[54] q_{eff} is given by

$$q_{eff} = \left(\frac{(\epsilon_0 - \epsilon_\infty)}{4\pi N} \hat{\mu} \omega_{TO}^2 \right)^{1/2} \frac{3}{2+\epsilon_0}, \qquad (10)$$

where ϵ_0 and ϵ_∞ are the static and optic dielectric

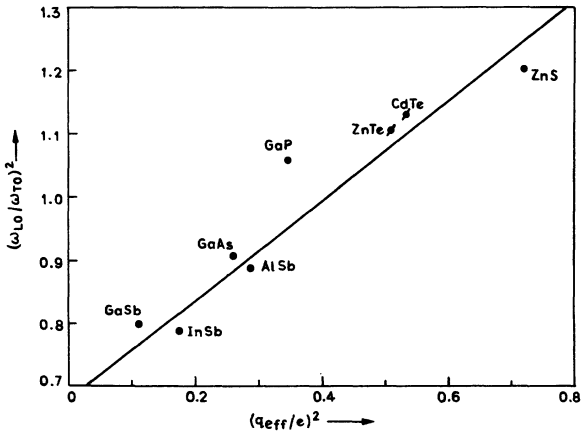

FIG. 7. Dependence of the ratio of longitudinal-optical frequency to transverse-optical frequency near the zone boundary on the effective charge in various zinc-blende semiconductors.

TABLE V. Effective ionic charges in zinc-blende-type crystals.

System	SNI model	Szigetti's relation
GaAs	0.567[a]	0.51[b]
AlSb	0.606[a]	0.53[b]
InSb	0.61[c]	0.42[b]
GaP	0.559[a]	0.58[d]
ZnS	0.934[e]	0.85[f]
SiC	1.049[e]	0.94[g]
ZnTe	0.77[c]	0.71[c]
CdTe	0.834[c]	0.72[c]

[a]Reference 16.

[b]M. Haas and B. W. Henvis, J. Phys. Chem. Solids 23, 1099 (1962).

[c]Present study.

[d]D. Kleinman and W. G. Spitzer, Phys. Rev. 118, 110 (1960).

[e]Reference 17.

[f]T. Deutsch, *Proceedings of the International Conference on the Physics of Semiconductors, Exeter, England*, 1962 (The Physical Society, London, England, 1962), p. 505.

[g]W. G. Spitzer, D. Kleinman, and D. Walsh, Phys. Rev. 113, 127 (1958).

constants, N is the number of ion pairs per unit volume, and $\hat{\mu}$ is the reduced mass of the two ions. This observation has been checked by Mitra[56] mainly for III-V semiconductors. In Fig. 7, we present the dependence of the ratio ω_{LO}/ω_{TO} (near the zone boundary) on the effective ionic charge, for a number of compounds, including II-VI semiconductors. The effective ionic charges calculated for the various II-VI and III-V compounds and other similar compounds using a SNI model are compared with those obtained by Szigetti's semiempirical formula [Eq. (10)] in Table V. A perusal of Table V reveals that the present model reproduces reasonable values for the effective charges. Keyes's idea that the two LO and TO branches will cross at the edge of the zone only for those systems which satisfy the inequality $q_{eff}/e \leq 0.7$ is also supported by the employed model.

V. DISCUSSION AND CONCLUSIONS

We have performed the lattice dynamics of zinc and cadmium tellurides on the basis of a second-neighbor-ionic model. The consistency of the calculated phonon frequencies has been checked by comparing them with the available optical data and by using the applicability of the Brout sum rule.[20] In interpreting the phonon peaks observed in infrared and/or Raman spectrum, most of the authors[25,51] have assigned values to the LO- and TO-phonon frequencies at the zone boundaries on the basis of their ionicity; i.e., it has been assumed that for the highly ionic crystals LO > TO, whereas for the less-ionic crystals, LO < TO. Recent neutron scattering data for the phonon frequencies for the highly ionic crystal ZnSe[4] and for the less-ionic crystal CuI[7] have manifested a totally different behavior from the aforementioned presumption. Therefore, in a situation when the exact critical-point-phonon frequencies are not known due to the nonavailability of the data by coherent-neutron spectrometry, a method employed in Sec. III for an approximate estimation of the zone-boundary-phonon frequencies LO and LA would be beneficial. The chosen phonon frequencies that reproduce the peak position observed in optical measurements with an accuracy of four wave numbers are very close to our lattice-dynamical calculated results. We may thus conclude that even in the absence of neutron scattering results, the structure of the observed absorption spectrum in zinc-blende-type crystals can be accounted for in terms of a set of phonon energies on the basis of a simple lattice-dynamical model.

ACKNOWLEDGMENTS

The authors wish to express their sincere thanks to Dr. Y. P. Varshni, Ottawa University, Canada, for providing us with details of their SNI model. One of us (D. N. T.) is thankful to Dr. P. N. Ram for helpful discussions. Financial assistance by Council of Scientific and Industrical Research and University Grants Commission, New Delhi, India, is also gratefully acknowledged. All the numerical calculations were performed on IBM 1401 and IBM 7044 computers installed at IIT, Kanpur.

[1]J. L. T. Waugh and G. Dolling, Phys. Rev. 132, 2410 (1963); G. Dolling and J. L. T. Waugh, *Proceedings of the International Conference on Lattice Dynamics, Copenhagen, Denmark*, 1963, edited by R. F. Wallis (Pergamon, London, 1965), p. 19.

[2]J. L. Yarnell, J. L. Warren, R. G. Wenzel, and P. J. Dean, Proceedings of the Conference on Inelastic Neutron Scattering, Copenhagen, Denmark, 1968 (unpublished).

[3]L. A. Feldkamp, G. Venktaraman, and J. S. King, Solid State Commun. 7, 1571 (1969); L. A. Feldkamp, thesis (University of Michigan, 1969) (unpublished).

[4]B. Hennion, F. Moussa, G. Pepy, and K. Kunc, Phys. Lett. 36A, 376 (1971).

[5]D. L. Price, J. M. Rowe, and R. M. Nicklow, Phys. Rev. B 3, 1268 (1971).

[6]C. Carabatos, B. Hennion, K. Kunc, F. Moussa, and C. Schwab, Phys. Rev. Lett. 26, 770 (1971).

[7]B. Hennion, F. Moussa, B. Prevot, C. Carabotos, and C. Schwab, Phys. Rev. Lett. 28, 964 (1972).

[8]W. Cochran, Proc. Roy. Soc. (London) A253, 260 (1959); Advan. Phys. 9, 387 (1960).

[9]J. L. Birman, Phys. Rev. 109, 810 (1958).
[10]H. M. J. Smith, Phil. Trans. Roy. Soc. (London) A241, 105 (1948).
[11]E. W. Kellerman, Phil. Trans. Roy. Soc. (London) A238, 513 (1940); Proc. Roy. Soc. (London) A178, 17 (1941).
[12]A. K. Rajagopal and R. Srinivasan, Z. Physik 158, 471 (1960).
[13]J. F. Vetelino and S. S. Mitra, Phys. Rev. 178, 1349 (1959).
[14]J. F. Vetelino, S. S. Mitra, O. Brafman, and T. C. Damen, Solid State Commun. 7, 1809 (1969).
[15]J. F. Vetelino, S. S. Mitra, and K. V. Namjoshi, Phys. Rev. B 2, 967 (1970).
[16]R. Banerjee and Y. P. Varshni, Can. J. Phys. 47, 451 (1969).
[17]R. Banerjee and Y. P. Varshni, J. Phys. Soc. Japan 30, 1015 (1971).
[18]D. N. Talwar and Bal K. Agrawal, Solid State Commun. 11, 1691 (1972).
[19]D. N. Talwar and Bal K. Agrawal (unpublished).
[20]R. Brout, Phys. Rev. 113, 43 (1959).
[21]L. Merten, Z. Naturforsch 13a, 662 (1958); 13, 1967 (1958); 17a, 174 (1962); 17, 216 (1962).
[22]R. Beserman and M. Balkanski (private communication).
[23]A. Hadni, J. Claudel, and P. Strimer, Phys. Status Solidi 26, 241 (1968).
[24]A. Manabe, A. Mitsuishi, and H. Yoshinaga, Japan J. Appl. Phys. 6, 593 (1967).
[25]S. Narita, H. Harada, and K. Nagasaka, J. Phys. Soc. Japan 22, 1176 (1967).
[26]R. E. Nahory and H. Y. Fan, Phys. Rev. 156, 825 (1967).
[27]O. Brafman, I. F. Chang, G. Lengyel, S. S. Mitra, and E. Carnall, Jr., Phys. Rev. Lett. 19, 1120 (1967).
[28]S. S. Mitra, J. Phys. Soc. Japan Suppl. 21, 61 (1966).
[29]H. D. Riccius, J. Appl. Phys. 39, 4381 (1968).
[30]P. Fisher and H. Y. Fan, Bull. Am. Phys. Soc. 4, 409 (1959).
[31]A. Mitsuishi, H. Yoshinaga, K. Yata, and A. Manabe, Japan J. Appl. Phys. 4, 581 (1965).
[32]A. Mitsuishi, US-Japan Cooperative Seminar on Far Infrared Spectroscopy, Columbus, Ohio, September 15–17, 1965 (unpublished).
[33]A. Mitsuishi, J. Phys. Soc. Japan 16, 533 (1963).
[34]C. J. Johnson, G. H. Sherman, and R. Weil, Appl. Opt. 8, 1667 (1969).
[35]O. M. Stafsudd, F. A. Haak, and K. Radisavljevic, J. Opt. Soc. Am. 57, 1475 (1967).
[36]G. L. Bottger and A. L. Geddes, J. Chem. Phys. 47, 4858 (1967).
[37]C. T. Senett, D. R. Bosoworth, W. Hayes, and A. R. L. Spray, J. Phys. C 2, 1137 (1969).
[38]G. A. Slack, F. S. Ham, and R. M. Chernko, Phys. Rev. 152, 376 (1966).
[39]G. A. Slack, S. Roberts, and J. T. Vallin, Phys. Rev. 187, 511 (1969).
[40]M. Haas and B. W. Henvis, J. Phys. Chem. Solids 23, 1099 (1962).
[41]J. Jouffroy, Compt. Rend. 265, 67 (1967); J. Pons-Corbeau and J. Jouffroy, Bull. Soc. Franc. Mineral Crist. 90, 498 (1967).
[42]M. Krauzman, Compt. Rend. B264, 530 (1967); 264, 1117 (1967).
[43]W. Taylor, Phys. Lett. 24A, 556 (1967).
[44]J. C. Irwin and J. LaCombe, J. Appl. Phys. 41, 1444 (1970).
[45]A. Mooradian and G. B. Wright, in *Ninth International Conference on Physics of Semiconductors*, edited by S. M. Ryvkin (Nauka, Leningrad, 1968), p. 1020. In the abstract of the paper the authors have given the values of phonon energies TA=35, LA=97, TO=151, and LO=118 cm^{-1} for CdTe. These values were corrected verbally because of the difficulty existing in the assignment to give TA=35, LA=97, TO=139, and LO=150 cm^{-1}.
[46]R. C. C. Leite and J. F. Scott, Phys. Rev. Lett. 22, 130 (1969).
[47]R. E. Halsted, M. R. Lorenz, and B. Segal, J. Phys. Chem. Solids 22, 109 (1961).
[48]J. L. Birman, Phys. Rev. 127, 1093 (1962); 131, 1489 (1963).
[49]G. A. Slack and S. Roberts, Phys. Rev. B 3, 2613 (1971).
[50]S. A. Solin and A. K. Ramdas, Phys. Rev. B 1, 1687 (1970).
[51]J. C. Irwin and J. LaCombe, Can. J. Phys. 48, 2499 (1970).
[52]S. S. Mitra, in *Optical Properties of Solids*, edited by S. Nudelman and S. S. Mitra (Plenum, New York, 1969), p. 333.
[53]S. S. Mitra and R. Marshall, J. Chem. Phys. 41, 3158 (1964).
[54]B. Szigetti, Trans. Faraday Soc. 45, 155 (1949).
[55]R. W. Keyes, J. Chem. Phys. 37, 72 (1962).
[56]S. S. Mitra, Phys. Rev. 132, 986 (1963).